2015

THE ROLE OF PROTEIN STRUCTURE CONFORMATIONAL CHANGE IN SECONDARY FUNCTIONS OF THREONYL-tRNA SYNTHETASE

Shawn Bruce Egri
University of Vermont

THE ROLE OF PROTEIN STRUCTURE CONFORMATIONAL CHANGE IN SECONDARY FUNCTIONS OF THREONYL-tRNA SYNTHETASE

A Defense Presented

by

Shawn B. Egri

at

The University of Vermont

In Partial Fulfillment of the Requirements
for College Honors
Specializing in Biochemistry

April 30, 2015

Examination Committee:

Christopher S. Francklyn, Ph.D., Advisor
Christopher C. Landry, Ph.D., Chairperson
Karen M. Lounsbury, Ph.D.

Acknowledgements

I am thankful for the support I received from all members of the Francklyn lab. To Dr. Christopher Francklyn who took me on in the fall of my senior year, who has supported me, and has shown me enthusiasm for this work. For Dr. Adam Mirando who has provided me with endless guidance in operating in the lab successfully. And lastly, thank you Jamie Abbott and Susan Robey-Bond for showing me positive attitude and curiosity throughout my time in lab.

Table of Contents

List of Abbreviations

AA: Amino acid

aaRSs: Aminoacyl-tRNA synthetases

BN: Borrelidin

CD: Circular dichroism

HPLC: High pressure liquid chromatography

IPTG: Isopropyl 1-thio-β-D-galactoside

T_m: Melting temperature

SDS-PAGE: Sodium dodecyl sulfate polyacrylamide gel electrophoresis

ThrRS: Threonyl-tRNA synthetase

TCA: Trichloroacetic acid

TNF-α: Tumor necrosis factor-α

VEGF: Vascular endothelial growth factor

VEGFR2: VEGF receptor 2

Abstract

Traditionally, threonyl-tRNA synthetase (ThrRS) has been studied for its canonical function of aminoacylation. Recently, however, the enzyme has been identified as a potent angiogenic factor. Both functions are influenced by a structural change within the enzyme. Upon binding of a specific inhibitor, borrelidin (BN), an alternative conformation is adopted, preventing angiogenic function. Mutant versions of ThrRS were generated using site-directed mutagenesis to mimic the BN-bound structure. The effects of these mutations on threonine-induced conformational changes were explored using steady state fluorescence. The greatest conformational impairment was seen with A460S and S488W which demonstrated 38% and 41% of the control response, respectively. Additionally, differential scanning fluorimetry was utilized to detail complex stabilization upon substrate binding. Specifically, the binding of threonine increased the melting temperature of the wild type enzyme by 9.82 °C, but had reduced effects on the other mutations, with S488W displaying the least (1.84 °C). Borrelidin binding was found to induce a biphasic melting trend for the wild type, S488W, and A460S constructs, in agreement with the proposed two-step binding mechanism by Ruan, *et al.* Future studies include: (i) investigating angiogenic potential of each construct using *in vivo* tube formation assay, and (ii) determining enzyme structure using X-ray crystallography.

I. Introduction

Aminoacyl-tRNA synthetases (aaRSs) are an important class of enzymes that catalyze the attachment of amino acids to their corresponding tRNA in a process known as aminoacylation. The product of this reaction, referred to as charged-tRNA, is subsequently targeted to the ribosome to donate amino acids to an emerging polypeptide, resulting in the formation of a functional protein [1]. For all aaRSs the generation of charged tRNA proceeds through a conserved, two-step mechanism:

$$E + AA + ATP \rightleftharpoons E \bullet AA\text{—}AMP + PP_i \qquad (1) – \text{Adenylate}$$

$$E \bullet AA\text{—}AMP + tRNA^{AA} \rightleftharpoons E + AA\text{—}tRNA^{AA} + AMP \qquad (2) – \text{Aminoacyl-tRNA}$$

In the first step of the reaction, known as activation, the amino acid (AA) is condensed with ATP to form an aminoacyl-adenylate intermediate. The formation of the adenylate species prepares the amino acid for its subsequent transfer to the terminal 2’ or 3’ hydroxyl group of the awaiting tRNA molecule. In addition to performing this important biological process, many aaRSs provide non-traditional secondary functions to the cell as well.

Recently, a growing body of evidence has revealed a diverse set of secondary functions among aaRSs: RNA splicing activity, transcriptional regulation, and stress signals including apoptosis and inflammation [1]. For instance, leucyl-tRNA synthetase possesses splice activity associated with excision of group I introns [2]. A second example is glutaminyl-tRNA synthetase, which operates to oppose a pro-apoptotic signaling pathway initiated by apoptosis signal-regulating kinase 1 [3]. Threonyl-tRNA synthetase (ThrRS) serves as a pro-angiogenic factor in response to specific signaling molecules in the cell [4].

Angiogenesis is a process of new blood vessels formation from pre-existing ones. The regulation of this effort is governed by the balance of positive and negative signals. Under normal conditions, blood vessels will release angiogenesis-inhibitory factors, such as angiopoetin-1 to maintain a quiescent state. However, in response to hypoxia, inflammation, or wound healing cells will release pro-angiogenic growth factors and chemokines. The most important of these signals is vascular endothelial growth factor (VEGF) which binds to the VEGF receptor 2 (VEGFR2) and activates downstream signaling cascades involved in the proliferation and migration of endothelial cells. Interestingly, in a recent study we have demonstrated that exposure of cells to VEGF or tumor necrosis factor-α (TNF-α) will stimulate the release of ThrRS in the extracellular space [4]. Furthermore, *in vitro* assays showed that adding exogenous ThrRS to low serum media in endothelial cell tube assays resulted in a significant increase in blood vessel branching and generation. It has been proposed that ThrRS promotes angiogenesis via induction of endothelial cell migration.

Suppression of blood vessel development has important implications in the fight against cancer. Initially the growth of many tumors is restricted by apoptosis associated with the hypoxic and nutrient deprived state of the tissue. However, eventually a small population of cells within the tumor acquires the ability to stimulate the growth of new capillaries and alleviate the former growth restraint. Referred to as the "angiogenic switch" this sudden increase in tumor vascularity provides the nutrients and migration capacity required for metastatic progression. Because angiogenesis is one of the key processes assisting transformation of cancer from the benign to malignant state, inhibition of ThrRS has important pharmaceutical implications [5]. When ThrRS is inhibited by the naturally-occurring antibiotic, borrelidin (Figure 1) (BN), metastasis can be suppressed [6-8].

Inhibition of ThrRS by BN displays noncompetitive kinetics. Binding occurs in a biphasic manner, with the second step resulting in enzyme isomerization and ultimately taking a longer time. This mechanism of inhibition is classified as a slow, tight binding inhibitor [9]:

$$E \underset{k_2}{\overset{k_1[I]}{\rightleftharpoons}} EI \underset{k_4}{\overset{k_3}{\rightleftharpoons}} E^{*}I$$

In this scheme EI is classified as the encounter complex, which forms under rapid equilibrium, and $E^{*}I$ represents the slow forming, higher affinity enzyme-inhibitor complex. The affinity of BN for ThrRS is extremely high: $K_i^{app} = 3.7 \pm 0.3$ nM [10].

Although BN binding displays noncompetitive kinetics, its mechanism resembles competitive modality. The binding of BN to ThrRS occurs in quadrivalent fashion. Occlusion of all three substrate binding sites occurs. Furthermore, the C4-C14 moiety of BN infiltrates a hydrophobic pocket adjacent to the active site [11]. During uninhibited conditions the threonine—ThrRS interaction elicits a "closing" of the enzymatic cleft, resulting in a 14° geometrical shift in an active site α-helix (residues D431-N448) (Figure 2) [11]. However, the presence of BN will induce a geometrical shift in the opposite direction. This results in a "locking" of ThrRS in its native conformation.

Examining the cleft closure associated with binding of canonical substrate is of current interest. It is unknown if this conformational change is crucial for effective aminoacylation activity of the enzyme. When BN is present, the conformational change is not permissible and thus aminoacylation cannot occur. However, it is not clear if this is due to the steric hindrance of the large, 18-carbon macrolide inhibitor. By locking the enzyme in the inhibited conformation, without the presence of BN, it can be examined as to how crucial the "closing" of the enzymatic

cleft is. Understanding this mechanism of inhibition is significant due to the severe toxicity of BN [12]. Although BN will inhibit the pro-angiogenic function of ThrRS, it also prevents functional aminoacylation. In recent studies this has led to death of the organism by way of the amino acid starvation response [12]. Alternative drug therapies have been developed to inhibit ThrRS with regards to angiogenesis but still allow native aminoacylation activity to occur [12].

Locking ThrRS in its native conformation can be completed by substitution of a smaller residue with a bulkier amino acid, such as tryptophan, in to the enzymatic cleft. This insertion will behave as a "prop," preventing the enzymatic cleft from closing when canonical substrate is inserted. Mutant ThrRS will exhibit a conformation similar to the BN-inhibited wild type enzyme (Figure 3). Target ThrRS mutations were developed by utilizing work completed for human threonyl-tRNA synthetase (TARS) constructs: Q566W, A538W, and R442A [13]. Equivalent mutations were designed in *E. coli* ThrRS for this study using PyMOL.

Mutant constructs should not undergo a conformational change associated with the binding of canonical substrate, namely threonine. To investigate whether a conformational change occurs in the presence of substrate, steady state fluorescence was utilized [14]. Steady state fluorescence was used to measure the conformational change of the enzyme. This method monitors the fluorescence activity of a tryptophan residue (W434) located adjacent to the enzyme's core [14]. Fluorescence activity is a function of the chemical environment of this residue. When threonine binds to wild type ThrRS a structural change occurs, changing the chemical nature of the tryptophan residue, resulting in a fluorescence decrease, or quench.

In the presence of canonical substrate a conformational change of wild type ThrRS occurs to stabilize the complex. When the conformational change cannot occur enzyme stability

should not increase. To explore enzyme stability, differential scanning fluorimetry will be used [15]. With increased stability a higher melting point should be observed. For wild type this means a higher melting point should be observed when canonical substrate is bound. The mutant ThrRS constructs should not display this trend.

The rate of aminoacylation activity must be high enough such that the enzyme can cooperate with the activity of the ribosome and all other aaRSs during translation. Measuring the rate of this process can be completed by measuring the aminoacylation activity during steady state conditions [16]. It is predicted that the mutant enzymes will observe a diminished aminoacylation rate due to the inhibited conformational change.

The aforementioned substitutions were successful in diminishing the conformational change of the enzyme in response to threonine. As a result aminoacylation activity as well as Thr:ThrRS complex stability was decreased. This shows support for the necessity of the conformational change in normal functioning of the enzyme. Due to the presence of BN in the enzymatic cleft a conformational change of the enzyme is prevented and thus canonical activity is eliminated. Future studies on the effects of the ThrRS mutants on aminoacylation potential will be investigated using the *in vitro* tube formation assay [4].

II. Methods and Materials

Mutant ThrRS Design

Appropriate enzyme mutations were modeled using the PyMOL molecular graphics system [17]. All mutations were designed to disrupt the conformational change associated with aminoacylation of ThrRS. This was completed by substitution of a residue adjacent to the binding pocket with a bulkier amino acid. Human ThrRS mutants which have been previously found to produce similar conformational change disruption were utilized as a template for *E. coli* ThrRS mutant development [13]. Mutants developed included A460S, R363W, and S488W.

Site-Directed Mutagenesis

Mutations of the ThrRS enzyme were completed using the QuikChange II Mutagenesis kit provided by Agilent Technologies [18]. Forward and reverse primers were developed to encode the parent plasmid with the appropriate mutations. After the primers bound to the parent plasmid DNA elongation was completed using *PfuUltra* HF DNA polymerase by the PCR method. An important reagent for successful mutagenesis was the Quik-Solution, provided by the QuikChange II XL Kit. This prevents the plasmid from supercoiling during replication. Isolation of the mutant plasmid was completed by digestion of the parent plasmid by the endonuclease Dpn I. This process occurs by breakdown of plasmid strains which contain methylated nucleobases. To check for the presence of mutant plasmid following digestion, agarose gel (0.8%) electrophoresis was completed.

Mutant plasmid was transformed into *E. coli* competent cells (JM-109) (Promega). Uptake of mutant plasmid into the organism was accomplished by heat-shock at 42 °C for 50

seconds. Organism recuperation was required following heat-shock and was completed by using a 1 hour regrowth period in SOC medium at 37 °C. SOC medium contains glucose, ions, and polypeptides. Bacterial colonies were then generated on LB plates containing 10 mg/L tetracycline overnight (16-18 hours). Colonies were harvested and cultured in 5 mL LB/tet broth. Mini-prep was completed for each colony to harvest plasmid DNA. This process separates whole plasmid from the remainder of the organism, including fragmented nucleobases. Sequencing of the entire mutant gene was completed at the DNA Facility at the University of Vermont and was analyzed using Sequencher.

ThrRS Purification

Enzyme expression was regulated by the lac operon [19]. Mutant bacterial strains were cultured in 1.5 L of LB-broth at a tetracycline concentration of 10 mg/L to a cell density of A_{280} = 0.6. Induction of the ThrRS gene was completed for 5 hours using isopropyl 1-thio-β-D-galactoside (IPTG) at a concentration of 1 mM. A bacterial pellet was resuspended in sonication buffer (20 mM potassium phosphate buffer pH 8.0, 100 mM KCl, 35 mM imidazole, 5 mM β-ME). Cellular lysis followed by treatment of cellular debris with protamine sulfate (0.4%) was done to remove insoluble cellular components as well as nucleic acids. High pressure liquid chromatography (HPLC) purified ThrRS product from other proteins. Purified ThrRS products contain a His_6-tag on their N-terminal end to permit chelation to a Ni-affinity column. Protein elution was completed using an imidazole gradient from 35 to 250 mM. Fractions were analyzed for the protein of interest using 8% SDS PAGE gels. ThrRS-containing fractions were pooled and dialyzed to remove imidazole. Enzyme concentration was completed using a 35000-MWCO membrane filter. Isolated protein was mixed with equivolume 80% glycerol for -20 °C storage.

A quantification of the enzymatically available active sites was measured by an active site titration, as described previously [16].

Steady-State Fluorescence

Intrinsic tryptophan fluorescence was measured using PTI technologies fluorimeter [14]. An excitation wavelength of 290 nm and an emission wavelength of 320 nm were used. ThrRS was suspended in a fluorescence buffer (20 mM Tris pH 7.5, 150 mM KCl, 15 mM $MgCl_2$, 5 mM β-ME) which was bubbled with argon gas prior to measurements. Measurements were made at an enzyme concentration of 100 nM; baseline enzyme fluorescence was equal to ~12-13x background. A titration of threonine over a range of 0.2-5.0 times the K_D (K_D=215 μM) was completed [14]. Consistent mixing was achieved using uniform pipetting after each addition of threonine. Measurements were made for 60 seconds at 1 count/sec. The average fluorescence value was calculated for each 60 sec measurement. Background and volume corrections ($V_{final}/V_{initial}$) were completed for each measurement and then corrected for unity. A plot of protein fluorescence (a.u.) versus threonine concentration (μM) was generated using data collected in triplicate and fitted with a best-fit line using the Prism graphing software.

Differential Scanning Fluorimetry

Enzyme stability was determined by measuring the melting temperature (T_m) of native and substrate-bound forms of ThrRS [15]. A fluorescently active dye, Sypro Orange, will produce signal upon binding to hydrophobic regions of the enzyme. At room temperature the hydrophobic regions of the enzyme are not accessible and thus a fluorescence signal will not be observed. A gradual increase in temperature (1 °C/min) was applied to the enzyme. At a well-defined temperature protein unfolding occurred and the dye bound to the enzyme. An increase in fluorescence intensity was observed at the temperature at which the enzyme denatured (T_m).

Melting point measurements were recorded for each enzyme in the presence of various substrates, including: threonine (5 mM), ATP (5 mM), BN (10 mM), and DMSO (which serves as the vehicle for BN). Binding of standard substrates, like Thr and ATP, were predicted to induce a conformational change of the enzyme, resulting in an increase of enzyme stability and thus an increase in T_m. The mutant enzymes wer predicted to not be able to undergo the same conformational change, and thus enzyme stabilization should not occur. The effect of borrelidin binding on the stability of the enzyme was measured using this method as well. It was predicted that borrelidin will increase the stability of the enzyme due to its tendency to lock the enzyme in a rigid conformation.

$tRNA^{Thr}$ Preparation

E. coli BL2(DE3) (New England Biolabs) cells expressing the $tRNA^{Thr}$-containing plasmid, coding for *E.coli* $tRNA^{Thr}$, were cultured in LB broth supplemented with 100 mg/ml ampicillin to a cell density of $A_{280} = 0.6$. Expression of $tRNA^{Thr}$ was induced with 1 mM IPTG overnight. Centrifugation was completed to harvest bacterial cells. The pellets were resuspended in suspension buffer (20 mM Tris pH 7.5, 20 mM $MgCl_2$, 10 mM β-ME) and then agitated with equivolume phenol (pH = 4.8) to extract all RNA from the cells. The aqueous fraction was ethanol precipitated overnight, and extracted RNA was resuspended in 10 mM HEPES and 50% formamide. This solution was resolved using 8M Urea/10% polyacrylamide gel electrophoresis. The tRNA was identified by UV shadowing, electroeluted into 1x TBE buffer (0.45 M Tris base, 0.45 M boric acid, 8mM EDTA pH 8.0), and then ethanol precipitated. The tRNA pellet was resuspended in 10 mM HEPES and stored at -20°C. The active concentration of $tRNA^{Thr}$ was determined by the plateau charging assay [16].

Steady State Aminoacylation Assay

The aminoacylation activities of ThrRS constructs were determined using modifications to established steady state aminoacylation procedures [16]. Briefly, reaction mixtures consisted of 20 mM HEPES pH 8.0, 100 mM KCl, 10 mM $MgCl_2$, 5 mM β-mercaptoethanol, 2 mM ATP, 1 U pyrophosphatase (Roche), 80 µM threonine, 20 µM [^{14}C]-threonine, and 30 µM $tRNA^{Thr}$. Reactions were initiated with the addition of 10 nM ThrRS (quantified active sites) and run at 37°C. Aliquots were taken at varying time points and spotted onto Whatmann 3MM paper filters pre-soaked in 5% trichloroacetic acid (TCA). Upon completion, the filters were washed 3 times in excess TCA, once in 95% ethanol, and dried under a heating lamp. The formation of ^{14}Thr-$tRNA^{Thr}$ was detected by scintillation counter and the activity determined by linear regression of threonyl-$tRNA^{Thr}$ formed per active site per unit time.

III. Results

Purifying ThrRS Constructs

Gene mutations were introduced via nucleobase substitution using the site-directed mutagenesis QuikChange II XL kit. The presence of plasmid following digestion (by Dpn I) was verified by agarose (0.8%) gel electrophoresis, suggesting the introduction of a successful mutation (data not shown). Mutant genes were analyzed at the University of Vermont DNA facility using Sequencher. The only mutations present in the genes were the desired substitutions.

The mutant plasmids were transformed into *E. coli*. The ThrRS gene was regulated by the *lac* operon which was induced using IPTG. A Ni-affinity column was used to purify ThrRS. Sodium dodecyl sulfate polyacrylamide gel electrophoresis (SDS-PAGE) verified that the molecular weight of the product was 74 kDa, indicating the correct molecular weight and that premature cleavage had not occurred during translation (Figure 4).

Aminoacylation Activity

An active site titration was used to determine the percentage of enzymatically available active sites. This was measured by calculating the ratio of AMP produced at various kinetic time-points, to the total amount of ATP initially added. It was determined that the wild-type and A460S constructs were 86% and 91% active, respectively. The S488W mutant was observed to be 51% active. Because the R363W mutant was kinetically inert (0% active), due to R363 being a crucial residue for threonine stabilization during catalysis, the total concentration as determined by absorbance was used for activity determination.

The steady state aminoacylation assay was used to determine the activity of the enzymes. Measuring the rate of charged-tRNA production was determined by calculating the amount of charged tRNA produced per active site at various time points (0-3 min). This method was completed under conditions of excess canonical substrate. A linear trend in product formation was observed (*Figure 5*). Relative enzymatic rates were represented by the slope of the best-fit line. Each ThrRS construct was demonstrated to be enzymatically active, except for the R363W mutant, as expected. Wild type ThrRS exhibited active sites which produce charged-tRNA at the highest rate, while S488W and A460S showed slower production (*Table 1*).

Threonine-Induced Conformational Change

Monitoring the conformational change of ThrRS associated with threonine binding was completed using stopped flow fluorescence, namely intrinsic tryptophan fluorescence. A range of threonine concentrations equal to 0.2–5 times K_D (215 μM) was added to 100 μM enzyme. This resulted in a decrease, or quench, of total fluorescence intensity. Each measurement was background and volume corrected. Because this method is not absolute and collects relative data points it was important to correct measurements for unity in order to compile data sets.

Every addition of substrate resulted in a quench in fluorescence intensity. However, the magnitude of the fluorescence decrease was not uniform with equimolar additions of threonine. Shown in *Figure 6* is the titration curve for each enzyme. A saturation of the conformational change was observed with each ThrRS construct. The conformational change of each mutant was not as intense as was observed for wild type. This trend is emphasized in *Table 2* which quantifies the magnitude of the conformational change for each enzyme relative to wild type. The A460S mutant responded minimally to the presence of threonine (37.6%), while R363W observed the greatest conformational change (63.0%).

Enzyme Stability as a Function of Substrate-Binding

Monitoring enzyme stability was completed by measuring the melting temperature (T_m) of the enzymes in the presence of various substrates. These substrates included threonine and ATP (*Figure 7a-d*). An increase in T_m due to the presence of substrate indicated enzyme stabilization. This was observed with the binding of threonine. A maximum stabilization of the enzyme was observed with wild type, with a ΔT_m of 9.82 °C (*Table 3*). The S488W mutant was relatively unresponsive to threonine, which observed a ΔT_m of 1.84 °C. By this method, ATP and DMSO binding was found to not affect the melting temperature of the enzyme (*Table 4*).

BN binding was found to induce a biphasic melting pattern for all of the enzymes, except R363W ThrRS (*Figure 8*). This may be attributed to a two-step unfolding process, with each unfolding element occurring at a separate temperature. A best-fit line could not be adjusted to these data due to the limited mobility of this method, and thus T_m could not be calculated. Additionally, the A460S and WT enzymes observed nearly identical melting curves in the presence of BN. The fluorescence fluctuation, indicated with SEM error bars, is minimal for the BN melting curves.

IV. Discussion

Enzyme Structure

The production and purification of the S488W, A460S, and R363W ThrRS mutants was completed successfully. Verification of the molecular weights of these compounds by SDS-PAGE showed that premature cleavage of the enzyme had not occurred; a stop codon was not erroneously inserted during mutagenesis. Furthermore, a fluorescence quench was observed in the presence of threonine. A conformational change in response to canonical substrate indicates proper enzyme folding.

Activity site titration showed that the wild type and A460S active sites were active at ≥ 90%, and the S488W mutant was found to be 50% active. ThrRS exists as a dimer. The S488W mutation may have caused a disruption of the dimeric interface, resulting in 50% enzyme activity. Differential scanning fluorimetry also indicated a potential for misfolding with a more intense fluorescence signal at baseline. A greater density of hydrophobic residues was exposed in the native conformation. This may be due to the enzyme being partially unfolded. The possibility of disrupted dimeric interactions and/or improper folding of S488W will be investigated further by measuring the enzyme structure using circular dichroism (CD) and X-ray crystallography.

Inhibition Mechanism of Borrelidin Binding

The binding mechanism of BN has been proposed as slow, tight binding by Ruan *et al*. [10]. This is characterized by a two-step mechanism, described by an encounter, low-affinity complex followed by enzyme isomerization to form a much higher affinity complex [11].

Biphasic protein unfolding trends of the wild type-, S488W-, and A460S- ThrRS:BN complexes were consistent with this mechanism. Each unfolding event may correspond to an analogous binding phase.

An alternative trend was observed with the R363W:BN complex, however. This complex experienced monophasic melting. This may have been caused by the bulky nature and location of the substitution. This is located in the active site of the enzyme; concomitant with the binding site of BN. Due to the insertion of this bulky residue in to the binding pocket of BN full spectrum inhibition was not permissible. Because partial enzyme stabilization was observed in the presence of threonine, it is suggested that the encounter complex does form, however.

Substrate-Induced Stabilization was Reduced with Mutants

During the intrinsic tryptophan experiments, saturation of the conformational change was reached for each construct. However, the fluorescence quench was less intense for the mutants. These trends indicate a lesser conformational change induced upon threonine binding. The bulkier substitutions utilized for the A460S and S488W mutants behaved as a "prop," preventing full closure of the enzymatic cleft. This trend is identical to that observed with the wild type ThrRS:BN complex [10].

A diminished conformational change in response to threonine was also observed using differential scanning fluorimetry. Enzyme stabilization in the presence of threonine was greatest for wild type (9.82 °C). On the contrary, the S488W mutant observed< 2 °C stabilization. These results are in agreement with the intrinsic tryptophan fluorescence data. S488W did not undergo a large conformational change and thus was not able to stabilize its structure to the same degree

that wild type did. Again, the bulky substitution prevented enzymatic cleft closure, resulting in less of a conformational response to substrate.

Although the R363W mutant responded with the largest mutant conformational change, the complex was only stabilized by 3.38 °C, or 34% of wild type. The reason this mutant observed a large conformational change, which did not result in an equivalent stabilization of the complex, is because this mutation disrupts a key binding residue of threonine to the enzyme [20]. Destabilization of the binding complex had occurred. Partial binding of the amino acid resulted in a conformational change of the enzyme, but the incomplete bonding as well as the insertion a bulky residue into the binding pocket, prevented complete complex stabilization.

The conformational and stability trends of A460S are currently unexplainable with the current model. A conformational analysis indicated that the smallest degree of conformational change is occurring, whereas differential scanning fluorimetry showed that significant enzyme stabilization occurs in the presence of threonine (6.97 °C). This may have been due to the incorporation of a hydrophobic residue into the enzymatic cleft of the enzyme. The serine residue may be interacting with threonine to stabilize the complex. To investigate this further a titration of the enzyme with borrelidin will be completed using intrinsic tryptophan fluorescence.

Conclusions

The importance of the conformational change associated with canonical activity of ThrRS was investigated successfully in this study. A S488W and A460S substitution resulted in an enzymatic "prop," preventing the full conformational action of ThrRS. As a result enzyme stabilization in the presence of threonine, as well as aminoacylation activity was diminished. Additionally, the S488W mutation may have also resulted in the loss of positive cooperativity. It

was also shown that the R363W substitution prevented stabilization of the molecule, as well as induced a complete inhibition of canonical activity due to this being a key binding residue of threonine. Finally, although the conformational change induced by the A460S mutation was minimal, a large stabilization of the Thr:ThrRS complex had occurred. These are contradictory phenomenon. This will be investigated further using alternative titration approaches.

Future studies include investigating *in vitro* effects of these mutations on angiogenesis using the tube formation assay, as described by Williams, *et al*. [4] This assay will determine the vitality of the conformational change with regards to angiogenesis. It is predicted that because S488W resembles the BN-bound wild type complex it will display minimal angiogenic activity. Wild type and R363W constructs are expected to induce angiogenesis due to their conformational differences with inhibited ThrRS.

V. Tables and Figures

Figure 1. Planar depiction of the 18-membered macrolide inhibitor, borrelidin.

Figure 2. An extrusion of an active site helix is prevented when ThrRS is bound to BN (yellow). A conformational change of varying magnitude occurs during the binding of various substrates to ThrRS: threonine (cyan; PDB-1EVK), $tRNA^{Thr}$ (green; PDB-1QF6), a threonyl adenylate analogue (purple; PDB-1NYQ). An overall difference in the conformational change of this helix is observed to be 14°.

Figure 3. Native conformations of wild-type (left), inhibited (center), and S488W (right) ThrRS constructs. In the presence of threonine cleft closure occurs for WT; BN binding prevents this conformational change. S488W is designed to mimic the inhibited conformation.

Figure 4. An 8% SDS-PAGE gel indicated that isolated protein was the correct molecular weight (74 kDa) for each construct. Lane 1: wild type (2 mg/mL); Lane 2: S488W (2 mg/mL); Lane 3: A460S (2 mg/mL); Lane 4: R363W (2 mg/mL).

Figure 5. Aminoacylation activity of the ThrRS constructs in the presence of excess substrate. This assay was used to quantify the amount of charged-tRNA produced per quantified active site per unit time. Wild type ThrRS was the most active, S488W and A460S were comparable, and R363W was considered kinetically inert.

Figure 6. Intrinsic tryptophan fluorescence of the WT, S488W, A460S, and R363W ThrRS constructs in response to an increasing concentration of threonine. A fluorescence decrease, or quench, is characteristic of a conformational change upon substrate binding. The R363W mutant

displayed the most fervent conformational change relative to control, and A460S and S488W were comparable.

Figure 7a-d. Enzyme stability as a function of substrate present. The inflection point of the curve represents T_m of the complex. Data points were calculated using a 9-point SEM average for every degree Celsius from 26-95 °C. Reaction conditions are color coded as: blue: without substrate; red: Thr; green: ATP; purple: DMSO.

Figure 8. Melting curves for the ThrRS:BN complexes were indicative of a biphasic melting trend for WT (blue), S488W (red), and A460S (green). The R363W (purple) mutant was considered to be monophasic.

Table 1. Aminoacylation activity of the ThrRS constructs as quantified by the slope of the steady state fluorescence curves. A larger slope represents a faster production of charged tRNA. The relative percent of activity of each mutant is shown in relation to the rate of wild type.

Table 2. The magnitude of the conformational changes recorded for each enzyme in response to a titration of threonine. Mutant conformational changes are presented in reference to the conformational change of WT ThrRS (%).

Table 3. Effects of threonine binding on the stability of ThrRS was system dependent.

Table 4. Effects of ATP binding to the stability of the ThrRS constructs was negligible.

Figure 1

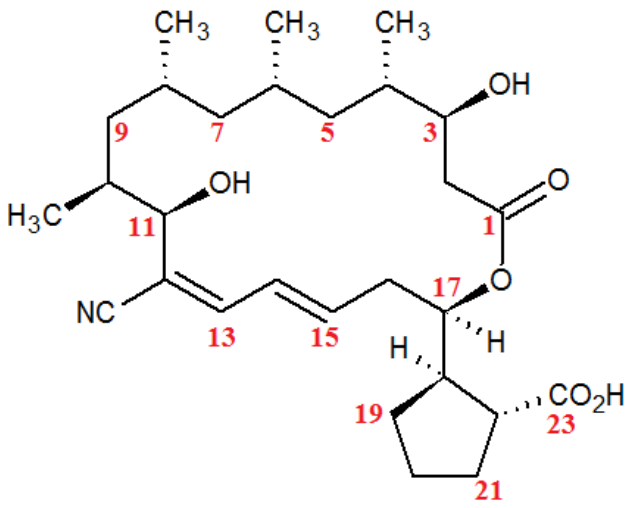

Figure 2

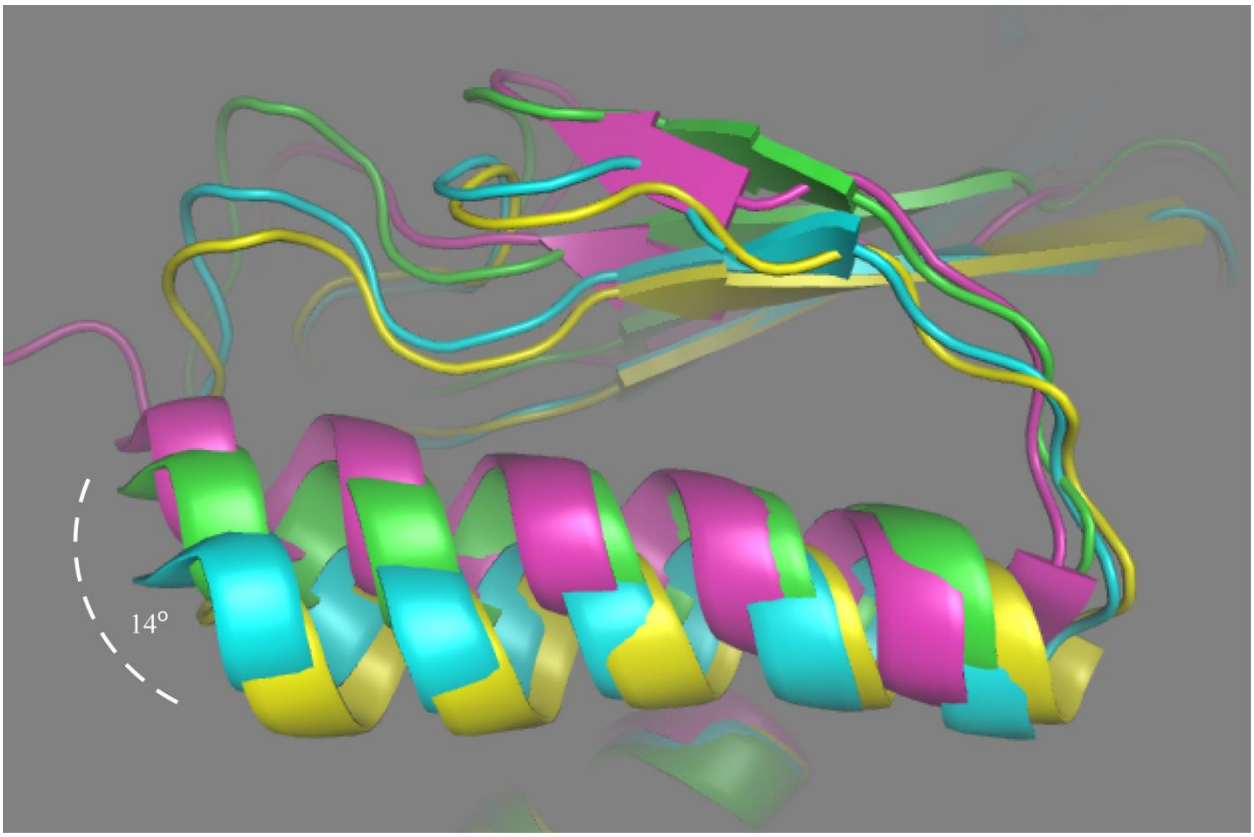

Figure 3

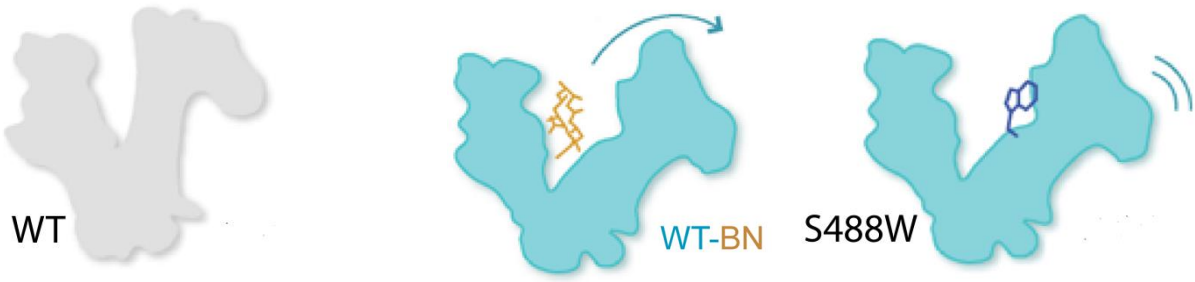

Figure 4

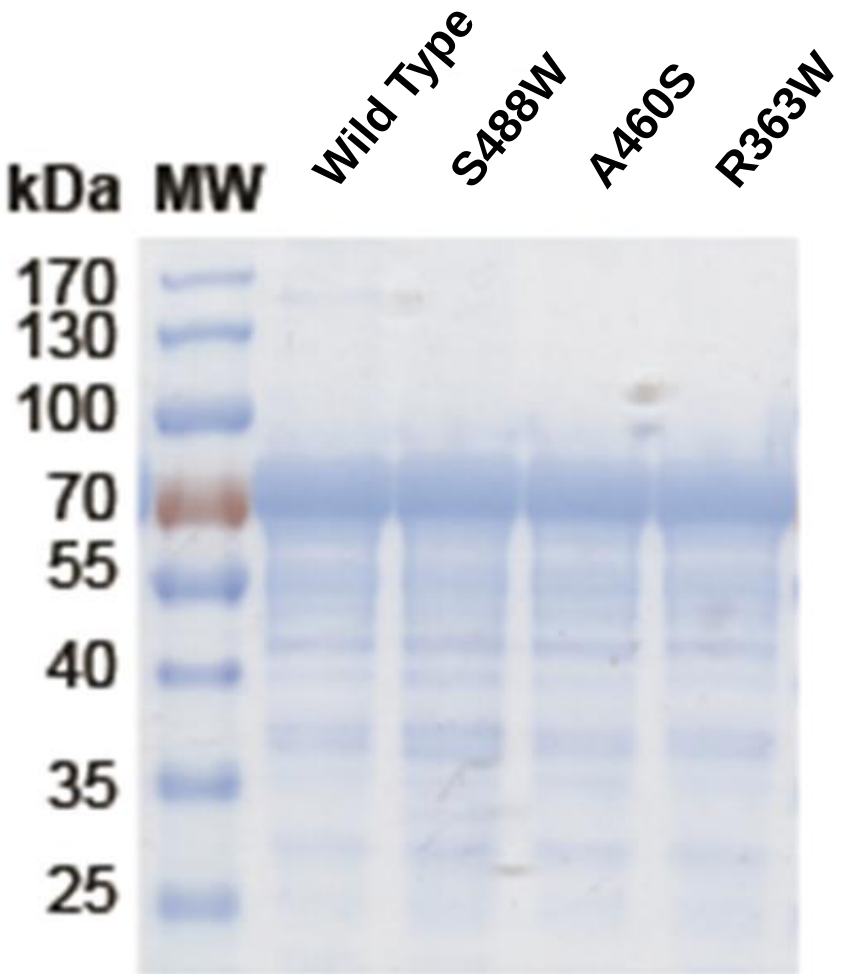

Figure 5

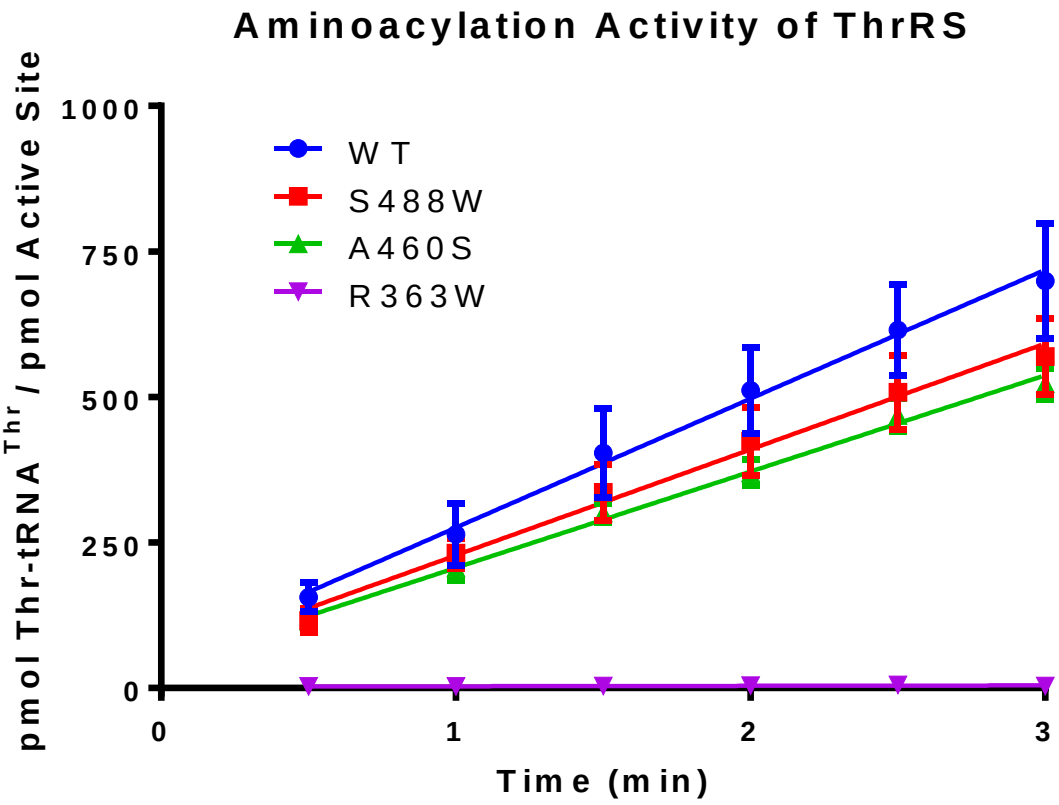
Aminoacylation Activity of ThrRS
pmol Thr-tRNA Thr / pmol Active Site
1000
750
500
250
0
0
1
2
3
Time (min)
WT
S488W
A460S
R363W

Figure 6

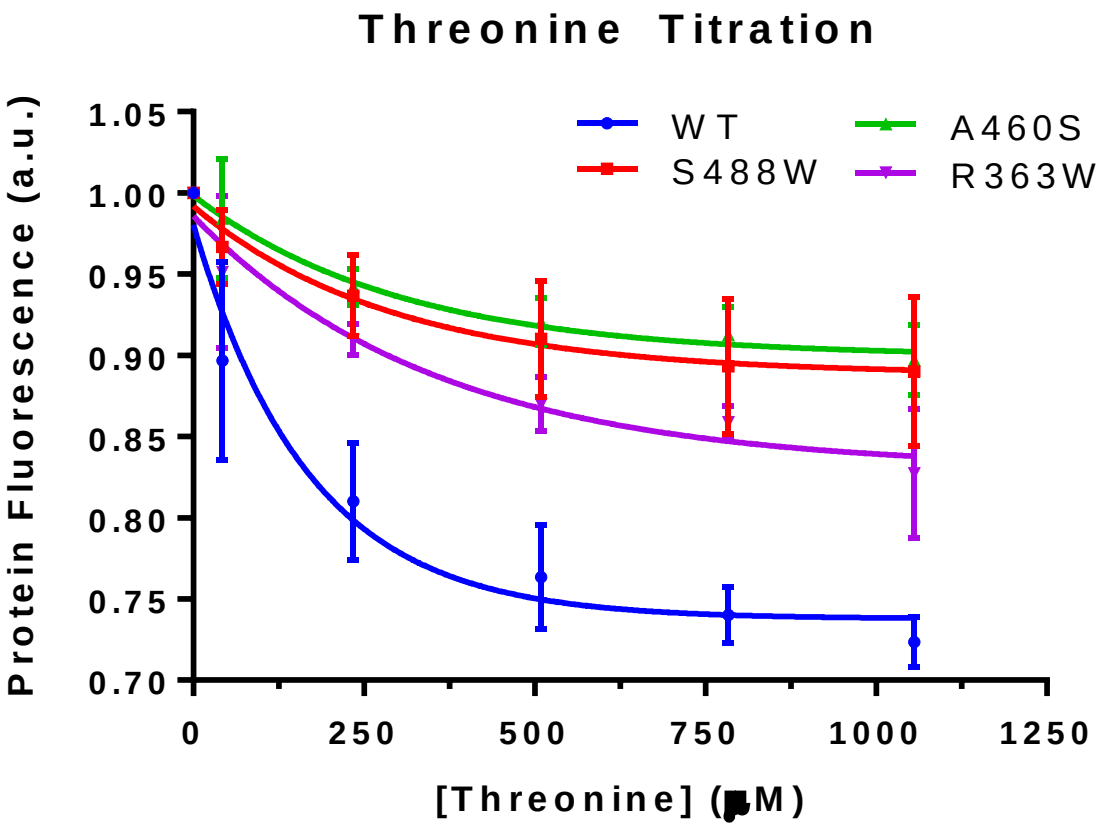
Threonine Titration
WT
A460S
S488W
R363W
Protein Fluorescence (a.u.)
1.05
1.00
0.95
0.90
0.85
0.80
0.75
0.70
0
250
500
750
1000
1250
[Threonine] (μM)

Figure 7a

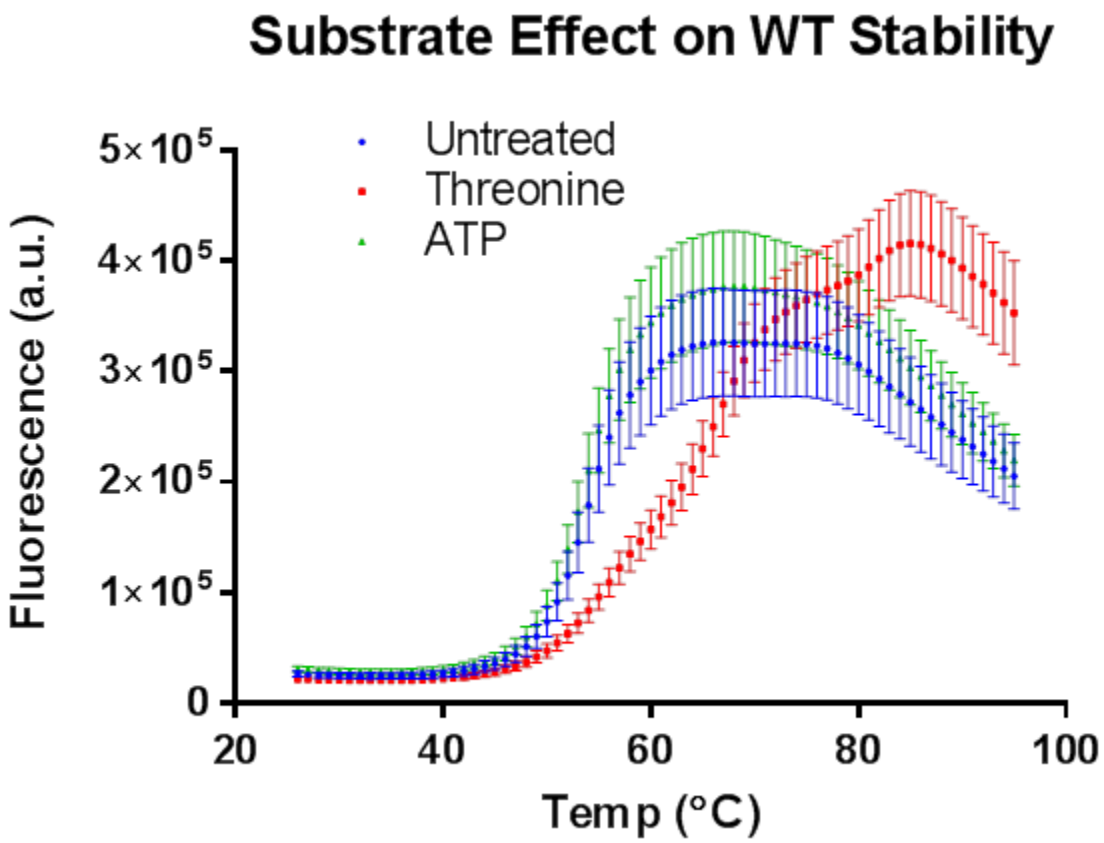
Substrate Effect on WT Stability
Untreated
Threonine
ATP
Fluorescence (a.u.)
5×10^5
4×10^5
3×10^5
2×10^5
1×10^5
0
20
40
60
80
100
Temp (°C)

Figure 7b

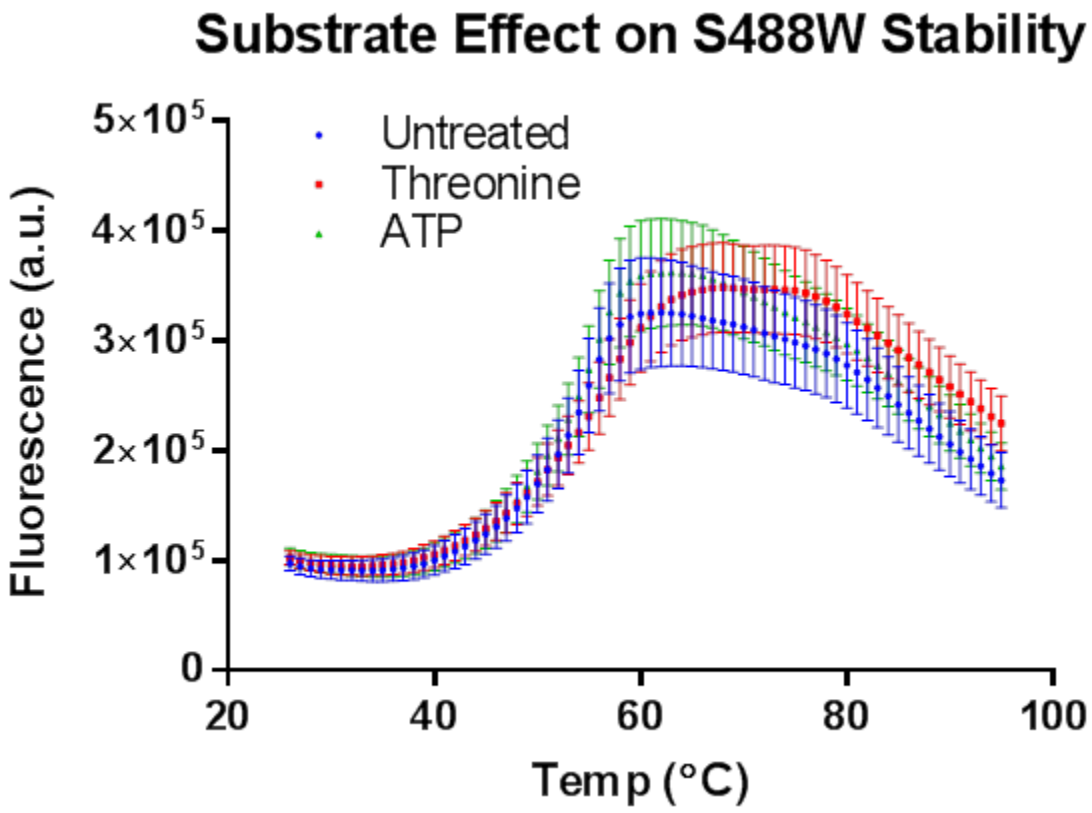
Substrate Effect on S488W Stability
Fluorescence (a.u.)
5×10^5
4×10^5
3×10^5
2×10^5
1×10^5
0
Untreated
Threonine
ATP
20
40
60
80
100
Temp (°C)

Figure 7c

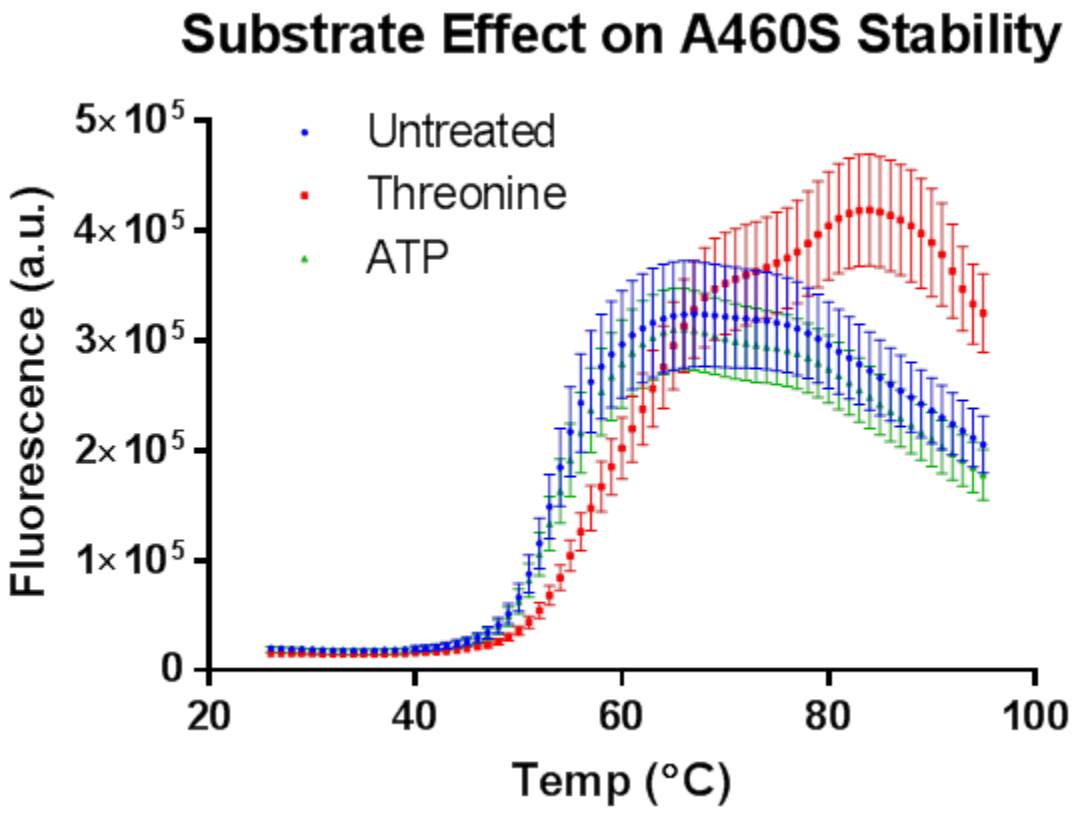
Substrate Effect on A460S Stability
Untreated
Threonine
ATP
Fluorescence (a.u.)
5×10^5
4×10^5
3×10^5
2×10^5
1×10^5
0
20
40
60
80
100
Temp (°C)

Figure 7d

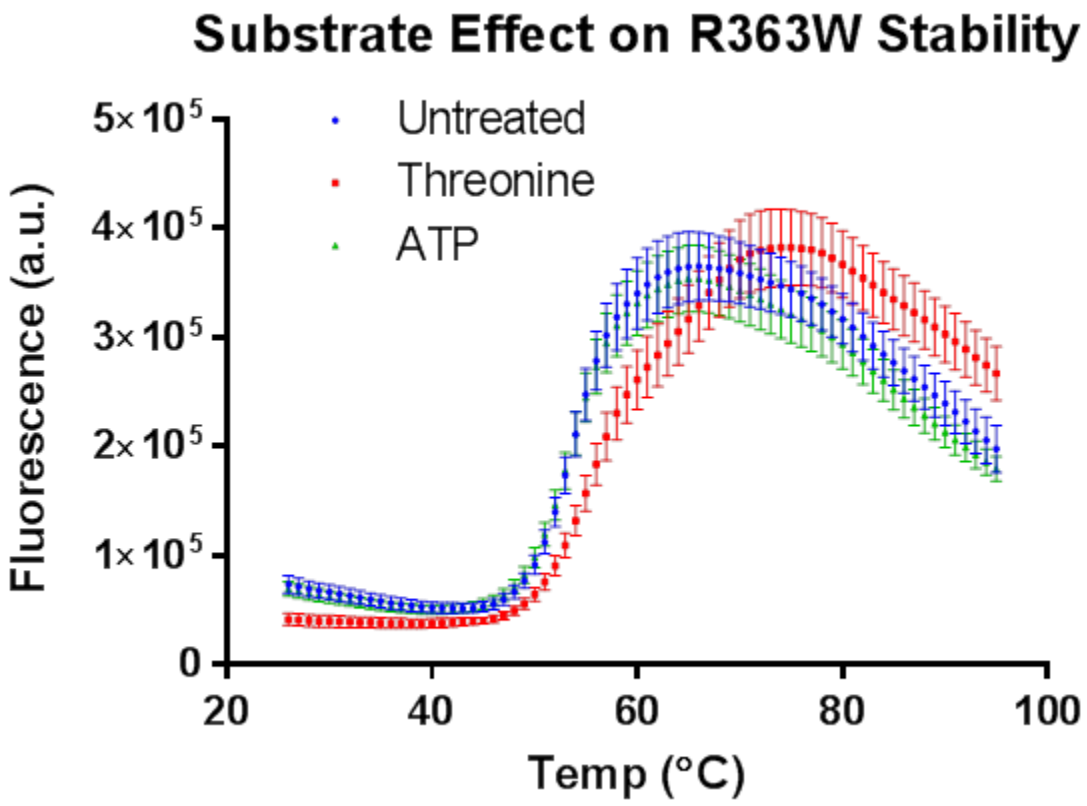
Substrate Effect on R363W Stability
Untreated
Threonine
ATP
Fluorescence (a.u.)
5×10^5
4×10^5
3×10^5
2×10^5
1×10^5
0
20
40
60
80
100
Temp (°C)

Figure 8

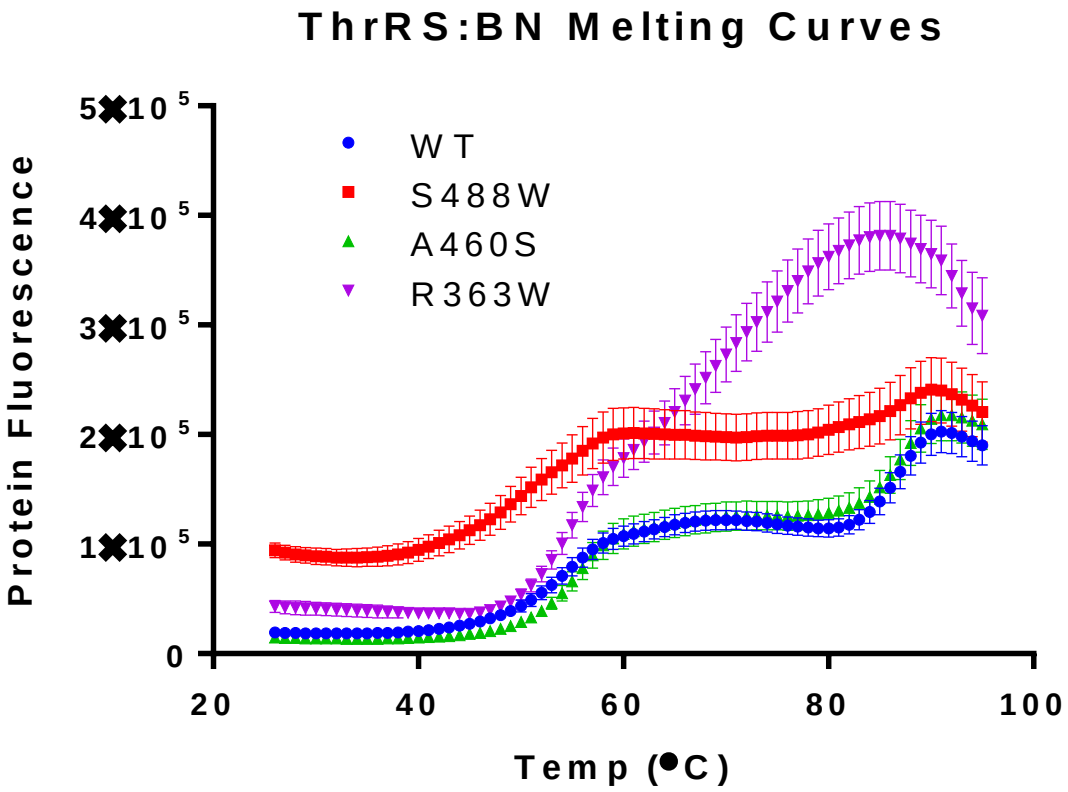
ThrRS:BN Melting Curves
Protein Fluorescence
5✖10 5
4✖10 5
3✖10 5
2✖10 5
1✖10 5
0
WT
S488W
A460S
R363W
20
40
60
80
100
Temp (●C)

Table 1

	WT ThrRS	**S488W ThrRS**	**A460S ThrRS**	**R363W ThrRS**
Slope	221.6 ± 17.65	182.1 ± 12.89 (82%)	165.5 ± 6.049 (75%)	0.749 ± 0.809

Table 2

Enzyme	Δ(a.u.)	% of WT
WT	0.27	100.00
S488W	0.11	40.79
A460S	0.10	37.57
R363W	0.17	62.98

Table 3

E. coli	Untreated	Thr	ΔT_m
WT	53.26	63.08	9.82
S488W	50.56	52.4	1.84
A460S	53.09	60.06	6.97
R363W	53.18	56.56	3.38

Table 4

E. coli	Untreated	ATP	ΔT_m
WT	53.26	53	- 0.26
S488W	50.56	50.75	0.19
A460S	53.09	53.5	0.41
R363W	53.18	52.71	-0.47

Literature Cited

1. Mirando, A.C., C.S. Francklyn, and K.M. Lounsbury, *Regulation of angiogenesis by aminoacyl-tRNA synthetases.* Int J Mol Sci, 2014. **15**(12): p. 23725-48.
2. Li, G.Y., et al., *In vitro mutagenesis of the mitochondrial leucyl tRNA synthetase of Saccharomyces cerevisiae shows that the suppressor activity of the mutant proteins is related to the splicing function of the wild-type protein.* Mol Gen Genet, 1996. **252**(6): p. 667-75.
3. Ko, Y.G., et al., *Glutamine-dependent antiapoptotic interaction of human glutaminyl-tRNA synthetase with apoptosis signal-regulating kinase 1.* J Biol Chem, 2001. **276**(8): p. 6030-6.
4. Williams, T.F., et al., *Secreted Threonyl-tRNA synthetase stimulates endothelial cell migration and angiogenesis.* Sci Rep, 2013. **3**: p. 1317.
5. Folkman, J., *Fighting cancer by attacking its blood supply.* Sci Am, 1996. **275**(3): p. 150-4.
6. Funahashi, Y., et al., *Establishment of a quantitative mouse dorsal air sac model and its application to evaluate a new angiogenesis inhibitor.* Oncol Res, 1999. **11**(7): p. 319-29.
7. Habibi, D., et al., *Borrelidin, a small molecule nitrile-containing macrolide inhibitor of threonyl-tRNA synthetase, is a potent inducer of apoptosis in acute lymphoblastic leukemia.* Invest New Drugs, 2012. **30**(4): p. 1361-70.
8. Harisi, R., et al., *Differential inhibition of single and cluster type tumor cell migration.* Anticancer Res, 2009. **29**(8): p. 2981-5.
9. Copeland, R.A., *Evaluation of Enzyme Inhibitors in Drug Discovery*. Methods of Biochemical Analysis. Vol. 46. 2005: Wiley-Interscience.
10. Ruan, B., et al., *A unique hydrophobic cluster near the active site contributes to differences in borrelidin inhibition among threonyl-tRNA synthetases.* J Biol Chem, 2005. **280**(1): p. 571-7.
11. Fang, P., et al., *Structural basis for full-spectrum inhibition of translational functions on a tRNA synthetase.* Nat Commun, 2015. **6**: p. 6402.
12. Mirando, A.C., et al., *Aminoacyl-tRNA synthetase dependent angiogenesis revealed by a bioengineered macrolide inhibitor.* Scientific Reports, Submitted.
13. Mirando, A.C., *CHARACTERIZATION OF A NON-CANONICAL FUNCTION FOR THREONYL-tRNA SYNTHETASE IN ANGIOGENESIS*, in *Department of Biochemistry*. 2015, University of Vermont.
14. Bovee, M.L., M.A. Pierce, and C.S. Francklyn, *Induced fit and kinetic mechanism of adenylation catalyzed by Escherichia coli threonyl-tRNA synthetase.* Biochemistry, 2003. **42**(51): p. 15102-13.
15. Niesen, F.H., H. Berglund, and M. Vedadi, *The use of differential scanning fluorimetry to detect ligand interactions that promote protein stability.* Nat Protoc, 2007. **2**(9): p. 2212-21.
16. Francklyn, C.S., et al., *Methods for kinetic and thermodynamic analysis of aminoacyl-tRNA synthetases.* Methods, 2008. **44**(2): p. 100-18.
17. DeLano, W.L., *PyMOL: An Open-Source Molecular Graphics Tool*, in *DeLano Scientific*. 2002, DeLano Scientific: San Carlos, California.

18. Wang, H., et al., *An efficient approach for site-directed mutagenesis using central overlapping primers.* Anal Biochem, 2011. **418**(2): p. 304-6.
19. Hansen, L.H., S. Knudsen, and S.J. Sorensen, *The effect of the lacY gene on the induction of IPTG inducible promoters, studied in Escherichia coli and Pseudomonas fluorescens.* Curr Microbiol, 1998. **36**(6): p. 341-7.
20. Dock-Bregeon, A.-C., P. Romby, and M. Springer, *Threonyl-tRNA Synthetases: A Multifunctional Enzyme in E. coli*, in *The Aminoacyl-tRNA Synthetases*. 2004.